HHS Public Access

Author manuscript

Process Saf Environ Prot. Author manuscript; available in PMC 2015 July 15.

Published in final edited form as:

Process Saf Environ Prot. 2015 May ; 95: 93–101.

Numerical modeling of water spray suppression of conveyor belt fires in a large-scale tunnel

Liming Yuan[*] and **Alex C. Smith**

Mine Safety and Health Research, National Institute for Occupational Safety and Health, P.O. Box 18070, Pittsburgh, PA 15236, USA

Abstract

Conveyor belt fires in an underground mine pose a serious life threat to miners. Water sprinkler systems are usually used to extinguish underground conveyor belt fires, but because of the complex interaction between conveyor belt fires and mine ventilation airflow, more effective engineering designs are needed for the installation of water sprinkler systems. A computational fluid dynamics (CFD) model was developed to simulate the interaction between the ventilation airflow, the belt flame spread, and the water spray system in a mine entry. The CFD model was calibrated using test results from a large-scale conveyor belt fire suppression experiment. Simulations were conducted using the calibrated CFD model to investigate the effects of sprinkler location, water flow rate, and sprinkler activation temperature on the suppression of conveyor belt fires. The sprinkler location and the activation temperature were found to have a major effect on the suppression of the belt fire, while the water flow rate had a minor effect.

Keywords

Conveyor belt fires; Computational fluid dynamics; Water sprinkler systems; Flame spread; Ventilation

1. Introduction

A conveyor belt fire in an underground mine can lead to a catastrophic situation. For example, on January 19, 2006, an underground mine conveyor belt fire occurred at the Aracoma Alma No. 1 mine, located in Logan County, West Virginia. Two miners were fatally injured when they became separated from their crew while trying to escape from the fire.

Some mines use belt air to provide additional air quantity to working sections that would otherwise not be possible without such a system. If a mine uses belt air at the mining face and the belt catches fire, the toxic gases and smoke produced from the burning of the belt are carried to the face, exposing miners to potentially hazardous levels of toxic gases such as CO, HCl, SO_2, H_2S, and NO_x. Also, the smoke produced from the burning belt limits

[*]*Corresponding author*. Tel.: +1 412 3864961. Lcy6@cdc.gov (L. Yuan).

Disclaimer: The findings and conclusions in this report are those of the authors and do not necessarily represent the views of the National Institute for Occupational Safety and Health.

visibility for the miners, making it much more difficult to escape from the mine. Therefore, it is important to suppress and control the belt fire in a timely manner in order to prevent the fire from causing any harm to the miners and ensure they can evacuate safely from the mine.

The U.S. Code of Federal Regulations (30 CFR 75.1101-7, and 8) requires a fire suppression system in underground coal mines to protect the conveyor belt entry and the first 50 ft of belting from the drive. These regulations were promulgated prior to the permitted use of belt air at the face. When water sprinkler systems are used, the suppression process of a belt fire is complicated by the interaction between the airflow, the flame spread over the belt, and the water spray in the entry. Some large-scale experiments were conducted by NIOSH to evaluate the effects of air velocity, water sprinkler activation temperature, and a limited water application time on the effectiveness of water sprinkler fire suppression systems to extinguish conveyor belt fires (Rowland et al., 2011; Teacoach et al., 2011).

Several novel fire suppression systems such as fire-fighting foam, fire gel, and water mist systems have been evaluated for the suppression of conveyor belt fires in underground coal mines (Teacoach and Thomas, 2013). To develop a more effective fire protection system for the conveyor belt entry in an underground mine, more systematic engineering data are needed. These data should include the effects of sprinkler location, water flow rate, sprinkler activation temperature, water droplet size, water droplet velocity, spray angles etc. Although full-scale experiments can be conducted to obtain engineering data to develop guidelines for performance-based designs for the installation of mine fire suppression systems, these tests are both expensive and time-consuming. Computational Fluid Dynamic (CFD) modeling is well adapted to this situation and can provide insights into the complicated interaction between the conveyor belt fires and the mine ventilation airflow. These interactions have a direct impact on the performance of the fire suppression systems. Such modeling can be completed in a short time and at comparatively low cost and can be used in conjunction with full-scale experiments to develop more effective engineering designs for installation of mine fire suppression systems.

CFD is the application of numerical techniques to solve the Navier–Stokes equations for fluid flow. CFD modeling has been widely used in simulating the interaction between water spray or mist and a fire. Novozhilov et al. (1997, 1999) simulated the extinguishment of a wood fire with a water spray. They developed a relatively comprehensive model, combining the water spray model with a fire extinction model. Prasad et al. (1999, 2002) simulated water mist suppression of small-scale methanol liquid pool fires and large-scale compartment fires. Parametric studies were performed to optimize various water mist injection characteristics for maximum suppression. Hua et al. (2002) conducted a CFD study on the interaction of water spray with a fire plume. The effects of several important factors such as spray pattern, water droplet size, and water spray flow rate on the fire suppression mechanism were investigated. Their simulation results indicate that CFD modeling has the capability to reasonably capture the interactions between the water spray and the fire plume, taking in account the effects of momentum exchange, heat and mass transfer, as well as chemical reactions. Yao and Chow (2005) developed a thermal model to study the extinguishment of a polymethyl methacrylate (PMMA) fire by water spray. The effects of droplet size and velocity, external radiant heat flux, and specimen configuration on fire

suppression were investigated. Yoon et al. (2007) conducted a computational study of the effect of water spray characteristics on the suppression of a large-scale (2 m × 2 m) pool fire in a 10 m × 10 m × 10 m compartment. Nmira et al. (2009) investigated the efficiency of water mist systems in mitigating thermoplastic fires in a tunnel numerically. A parametric study was carried out to study the effects of ventilation rate, nozzle location, injection mass flow rate, and droplet size on the performance of water mist systems. Trelles and Mawhinney (2010) used the National Institute of Standards and Technology (NIST) Fire Dynamics Simulator (FDS) program to investigate a large-scale pallet stack fire in tunnels protected by water mist systems. An algorithm was developed to allow the fire to spread along the top of a series of pallet loads and the measured heat release rate (HRR) was reproduced. Blanchard et al. (2013) conducted experimental and numerical studies of the interaction between water mist and fire in an intermediate test tunnel. An extensive numerical study using FDS was conducted to quantify each mechanism involved in interaction between water mist and hot gases. Finally, Jenft et al. (2014) conducted numerical simulations with FDS to study the suppression of a pool fire using water mist.

Although much research has been done to model fire suppression using water spray or water mist, limited research has been conducted specifically to simulate the suppression of conveyor belt fires using water spray. The purpose of this study is to simulate the water spray suppression of conveyor belt fires in a large-scale tunnel with ventilation. The flame spread over the conveyor belt was modeled to reflect the real development of the belt fire. The CFD model was calibrated using large-scale experimental results. The calibrated model was used to investigate the effects of sprinkler location, water flow rate, and sprinkler activation temperature on the suppression process. The simulation results can be used to design more effective fire protection systems for the conveyor belts used in underground coal mines.

2. Modeling of water spray suppression

To simulate the water spray suppression of conveyor belt fires, the flame spread over the conveyor belt needs to be modeled first. In a previous study (Yuan et al., 2014), the flame spread over the conveyor belt in a large-scale tunnel was simulated using FDS. Thermogravimetric analysis (TGA) data for the conveyor belt was used to determine the kinetic properties for modeling the pyrolysis process of the conveyor belt burning. The CFD model was calibrated using large-scale conveyor belt fire test results. The comparison between simulation and test results showed that the CFD model was able to capture the major features of the flame spread over the conveyor belt.

In the current study, FDS is again used to simulate the water suppression of conveyor belt fires. FDS has previously been used to simulate the performance of water spray and mist fire suppression systems successfully (Vaari et al., 2012; Sikanen et al., 2014). To simulate water spray suppression of belt fires, some spray characteristics need to be specified as input for the simulations. Those characteristics include sprinkler activation temperature, sprinkler response time index (RTI), water flow rate, droplet diameter, droplet initial velocity, and spray angles. The sprinkler activation temperature and RTI value were obtained from the

sprinkler manufacturer. The water flow rate was calculated based on the K-factor value of the sprinkler and the operating pressure used in the test using the equation:

$$\dot{m}=K\sqrt{P} \quad (1)$$

where $\dot{m}$ is the water flow rate in liter/min (Lpm), K is the K-factor for the sprinkler in Lpm/bar$^{0.5}$, and P is the operating pressure in bar. A water spray usually consists of spherical droplets with various sizes. The size distribution of water droplets can be expressed in terms of its Cumulative Volume Fraction (CVF), a function that relates the fraction of the liquid volume transported by droplets less than a given diameter. The CVF for a sprinkler may be represented by a combination of log-normal and Rosin–Rammler distributions (McGrattan et al., 2010):

$$F(d)=\begin{cases} \frac{1}{\sqrt{2\pi}}\int_0^d \frac{1}{\sigma d'} e^{-\frac{\left[ln\left(d'/d_m\right)\right]^2}{2\sigma^2}} dd' & (d \le d_m) \\ 1-e^{-0.693\left(\frac{d}{d_m}\right)^{\gamma}} & d>d_m \end{cases} \quad (2)$$

where d_m in m is the median droplet diameter defined as the diameter of a droplet for which half of the droplets have a larger diameter and half a smaller diameter, and γ and σ are empirical constants equal to about 2.4 and 0.6, respectively. The median droplet diameter is a function of the sprinkler orifice diameter, operating pressure, and geometry. Research has found a correlation for the median droplet diameter (Lawson et al., 1988):

$$\frac{d_m}{D}=c\,We^{-1/3} \quad (3)$$

where D is the orifice diameter of the sprinkler in m and c is a constant. The Weber number, We, defined as the ratio of inertial forces to surface tension forces is given by

$$We=\frac{\rho_d u_d^2 D}{\sigma_d} \quad (4)$$

where ρ_d is the density of liquid in kg/m^3, u_d is the droplet initial velocityin m/s, and σ_d is the liquid surface tension in N/m. The initial velocity can be computed from the mass flow rate and the orifice diameter. The constant c in Eq. (3) appears to be independent of flow rate and operating pressure. Sheppard (2002) conducted an extensive experimental study to measure the water spray characteristics for fire sprinklers. The value for the constant c measured in his study ranged from 0.72 to 2.48 with an average of 1.53. The calculated median droplet diameter using Eq. (3) for the sprinkler used in this study, based on the Sheppard study average value, was 503 μm.

When water droplets encounter burning surfaces, the water not only cools the surface and the surrounding gas, but it also changes the pyrolysis rate of the fuel. In the FDS model, when a liquid droplet hits a solid horizontal surface, it is assigned a random horizontal direction and moves at a fixed velocity until it reaches the edge, at which point it drops straight down at the same fixed velocity. This “dripping” velocity has been measured for water to be on the order of 0.5 m/s. While attached to a surface, the “droplet” is assumed to

form a thin film of liquid that transfers heat from the flame to the solid, and heat and mass to the gas. In the FDS model, the cooling of unburned surfaces and the reduction in the Heat Release Rate (HRR) are computed locally. The exponential nature of suppression by water is observed both locally and globally; thus it is assumed that the local burning rate of the fuel can be expressed in the form (McGrattan et al., 2010)

$$\ddot{m}''_f(t) = \ddot{m}''_{f,0}(t) e^{-\int k(t) dt} \quad (5)$$

Here $\ddot{m}''_{f,0}$ is the burning rate per unit area of the fuel when no water is applied and k(*t*) is a linear function of the local water mass per unit area, m_w'',

$$k(t) - a\ddot{m}''_w(t) \quad (6)$$

where *a* is an empirical constant.

3. Large-scale conveyor belt fire suppression test

Results from a large-scale conveyor belt fire suppression test were used to calibrate the CFD model. The large-scale conveyor belt fire suppression test was conducted at the NIOSH Fire Suppression Facility (FSF). The FSF, shown in Fig. 1, is configured in a T shape to simulate a main mine entry and crosscut. For the conveyor belt fire suppression test, the crosscut was closed off. The main entry is 46.6 m long, 5.5 m wide, and 2.2 m high. The FSF is equipped with a 1.8-m-diam, variable speed axial vane fan, located at one end of the main tunnel to provide ventilation. The fan has a pneumatic controller to adjust the fan pitch in order to increase or decrease the air velocity.

The FSF is equipped with a nine-point gas monitoring array at the open end of the tunnel to measure the gas components produced from a belt fire test. The array is made of 1.3-cm-diam black steel pipe positioned at the center of the entry. A total of nine 0.3-cm holes are drilled into the vertical section of the pipe to sample the gases. The sample holes are equally spaced vertically from the roof to the floor. A 1.3-cm tube is connected to the steel pipe and leads back to the control room to a set of infrared gas analyzers. The gas analyzers measure carbon monoxide (CO), carbon dioxide (CO_2), and oxygen (O_2) gas concentrations. The gas data was collected every 2 s and was recorded by a computer-based data acquisition system.

The conveyor belt structure is located 26 m from the fan and is slightly off-center of the entry to allow for heavy equipment to pass on one side to place the belting onto the structure. The conveyor belt structure is 15 m long and 2.2 m wide. To ignite the belt, four sets of natural gas impinged jet burners, connected in series, were placed in front of the belt structure, as shown in Fig. 2. Each burner was equipped with 60 stainless steel jets, having a combined rated output of 44 to 114 kW per burner. The ignition region was confined by metal shields on the front, left, and right sides, and at the top to form a box around the ignition zone to reduce the effects of the ventilation on the ignition process (not shown in the figure). The back side was unshielded toward the open end of the fire tunnel.

The water sprinkler fire suppression system was installed over the conveyor structure in accordance with 30 CFR 75.1101-8. In this study, glass bulb-type sprinklers with an activation temperature of 140°C were used. The sprinklers were from a name brand manufacturer with a discharge coefficient of $K = 80.6$ Lpm/bar$^{1/2}$. Eight sprinklers were installed with the center distance of 2.4 m to protect 15.2 m of the structure along the centerline of the belt. The first sprinkler was located 0.7 m from the horizontal leading edge.

The conveyor belt used in this study is made of styrenebutadiene rubber (SBR). During the test, an 11.4-m-long, 1.8-m-wide, and 15-mm-thick piece of SBR conveyer belt was installed on the conveyor belt structure. The upstream end of the belt was affixed to the burners by metal wire, as shown in Fig. 2. Thermocouples were installed on the center line of the belt at 1.5-m intervals and along the two edges of the belt at 3-m intervals. The first row of thermocouples was placed 0.6 m from the front of the belt in the ignition zone. Each thermocouple was placed 2 mm below the surface of the belt to measure the belt temperature and determine when the flame reached that distance on the belt. The air velocity used in the test was 1.5 m/s and was measured using a handheld vane anemometer over the top center of the belt, 5 m beyond the ignition zone and 0.3 m above the surface of the belt. Air velocity measurements were also made at the thermocouple and gas points at the exit of the tunnel, 46 m from the fan. The exit air velocities at each point were averaged together and recorded as the exit air velocity.

In the test, the natural gas burners were ignited with a propane torch. The natural gas was allowed to flow for 10 min before it was turned off. The first sprinkler was activated 3.2 min after the gas burners were turned off. No other sprinkler was activated and the fire was extinguished.

4. Numerical details

Fig. 3 shows the physical model of the simulated tunnel and the conveyor belt. The dimensions for the actual tunnel are 46.6 m long, 5.5 m wide, and 2.2 m high. For the simulation the tunnel length was limited to 20 m. The metal shields used in the test to prevent the blowout of the ignition flame were modeled as the real sizes. The structure supporting the conveyor belt in the test was not modeled. The airflow velocity at the inlet of the tunnel was set at 1.5 m/s as in the test.

It is difficult to model the burning of the section of the belt with the burners on because of the complexity of the ignition process. In the simulation, the burning of the belt from the burners to the edge of the structure surface is not modeled; instead a vertical obstruction is placed from the leading edge to the floor. The burners are located on the floor between the shields and the obstruction. The average value of the measured HRRs when the burners are on is used as the heat output for the burner.

It is well known that grid size can affect the FDS simulation results. Therefore, it is important to determine an appropriate grid size to achieve desired reliability. As suggested by McGrattan et al. (1998), the grid size near the fire source should be no larger than $0.1D^*$ to ensure reliable simulation results. D^* represents the characteristic length scale for a fire source and is written as

$$D^* = \left(\frac{Q}{\rho C_p T_0 \sqrt{g}} \right)^{2/5} \quad (7)$$

where Q is HRR of fire in kW, ρ is air density in kg/m^3, C_p is air-specific heat in kJ/kg-K, T_0 is ambient temperature in K, and g is gravity acceleration in m/s^2. In our large-scale conveyor belt test, the measured HRR, Q, was between 2 and 7 MW. The corresponding value for D^* is between 1.3 and 2.1m. Therefore, a grid size of 0.1 m was selected in this study.

5. Results and discussion

5.1. Calibration of CFD model

Fig. 4 shows the comparison of HRRs between the test results and the simulation. Because the ignition process was not exactly modeled, the starting time for the comparison was chosen as the time that the surface temperature 2 m away from the leading edge of the belt started to increase in both the test and the simulation. In the test, when the sprinkler was activated the maximum HRR was 3.25 ±0.02 MW, while the maximum HRR was slightly above 3 MW in the simulation. Before the water sprinkler was activated, the HRR in the simulation was in good agreement with the test, while the HRR in the simulation dropped more quickly than in the test after the sprinkler activation. This is probably caused by the model's immediate reduction of pyrolysis by the water spray. It was observed in the test that the belt was still burning and smoldering 5 min after water droplets hit the fuel surface. This indicates that the reduction in pyrolysis caused by water droplets was slower than in the model.

Fig. 5 shows the comparison of belt surface temperature 4.5 m from the leading edge for the test and the simulation. The calculated surface temperature in the simulation at this location before the sprinkler activation was higher than in the test. After the sprinkler activation, the surface temperature dropped more quickly in the simulation than in the test, probably because of the same reason as for the HRR. These comparisons demonstrate that the CFD simulation of the water spray suppression of conveyor belt fires was able to capture the major features of the suppression process in terms of HRR reduction and belt surface temperature cooling after the sprinkler activation. The calibrated CFD model was used to investigate the effects of sprinkler location, water flow rate, and sprinkler activation temperature on the effectiveness of suppression of conveyor belt fires.

5.2. Effect of sprinkler location

The simulations were conducted to examine the effect of sprinkler location on the suppression of the belt fires. Under the requirements of 30 CFR Part 75.1101-8, at least one sprinkler shall be installed above each belt drive, belt take-up, electrical control, and gear-reducing unit, and individual sprinklers shall be installed at intervals of no more than 8 feet along all conveyor branch lines. In practice, the distance of 2.4m (8 ft) between two adjacent sprinklers is commonly used. As observed in the large-scale test, single sprinkler activation was enough to extinguish the conveyor belt fire if the sprinkler was activated before the

flame front passed the sprinkler water spray. Therefore, the location of the first sprinkler is very important. In this study, the location of the first sprinkler was changed from 0 to 2.4m with an increment of 0.3 m. The second sprinkler was always set at 2.4 m downwind from the first one. With different first sprinkler locations, the first sprinkler was always the only one activated except at the location exactly above the belt leading edge. When the sprinkler was set at exactly above the belt leading edge, the first sprinkler was never activated; instead the second one was activated and suppressed the fire. It should be pointed out that this happened at the airflow velocity of 1.5 m/s used in this study. For a lower airflow velocity, the result may be different.

The activation times for the first sprinkler at different locations are shown in Fig. 6. It is interesting to note that the sprinkler activation time decreased first with the distance from the belt leading edge, reached the minimum value of 152 s at the distance of 1.2 m, and then increased with the distance from the belt leading edge. The longest activation time occurred when the first sprinkler was set at 0.3 m from the belt leading edge. Fig. 7 shows the HRRs for sprinkler locations at 0.3 m, 1.2 m, and 2.4m, respectively. It should be pointed out that at the 1.2-m sprinkler location, the HRR was less than 2 MW when the sprinkler was activated, and there was no apparent HRR reduction after the sprinkler was activated. The value simply leveled off and fluctuated indicating that the flame never spread and the fire was not developed. By contrast, the HRR was reduced sharply when the sprinkler at 0.3-m location was activated. The HRR value was about 4.4MW at the activation, suggesting the flame had spread and the fire was well developed.

These results indicate that there are two modes of water spray suppression for conveyor belt fires. In the first suppression mode, the fire was suppressed before it was well developed and the HRR was low at the activation. Thus, there was no apparent HRR reduction after the water spray was activated. In the second suppression mode, the fire was suppressed after it was well developed and the HRR was relatively high. Thus, there was a significant HRR reduction after the spray activation on, as shown in Fig. 7 at the locations of 0.3 m and 2.4m.

The maximum HRRs before the sprinkler activation for different sprinkler locations are shown in Fig. 8. Although the trend in Fig. 8 is similar to the one in Fig. 6, only at two locations, 0.3 m and 2.4m, were the fires well developed before the spray was on, indicating that only at these two locations, the fires were suppressed with the second mode. Jenft et al. (2014) found the same two suppression modes in their experimental and numerical study of pool fire suppression using water mist. A fast suppression was observed when water mist was applied to a developed fire. When the mist was applied early, fire growth was controlled, but its suppression required a longer application and only occurred after a significant cooling of the flame and the liquid pool.

To further explore the differences between the two fire suppression modes, the centerline belt surface temperatures 5 m from the belt leading edge at different sprinkler locations are plotted in Fig. 9. At locations of 0.3 m and 2.4m, the fire was well developed and the flame already reached the 5-m position, and the surface temperature there was well above 500°C. After the spray activation, the temperature was reduced quickly. At other sprinkler locations, the surface temperatures before the spray activation were much lower, and the flame did not

spread to the 5-m position. Interestingly, the surface temperatures for locations of 0.3 m and 2.4m eventually fell below the temperatures for other sprinkler locations.

Fig. 10 compares the centerline surface temperatures 7 m from the belt leading edge for different sprinkler locations. At sprinkler locations of 0.9 m, 1.2 m, 1.5 m, and 1.8 m, the temperature still increased slowly after the sprinkler activation, while the temperature continually decreased at other sprinkler locations. Considering the potential for the belt to reignite, those cases with increasing surface temperatures after sprinkler activation are considered as a failure of fire suppression.

Fig. 11 compares the smoke temperatures 15 cm below the roof downstream of the belt for different sprinkler locations. The smoke temperature for sprinkler location of 0.3 m had a highest value when the spray was on; however, the value decreased quickly below the temperatures for all other sprinkler locations, indicating that there was a more significant gas-phase flame suppression caused by the highest HRR before the spray was on at this sprinkler location. This also can be evidenced from the radiation heat loss plotted in Fig. 12 for sprinkler locations of 0.3 m, 1.2 m, and 2.4 m. At the 0.3-m location, the radiation heat loss dropped quickly below the values of the other two locations after the spray was on.

When the first sprinkler was set at exactly above the belt leading edge, the first sprinkler was never activated, while the second one that was 2.4m apart from the first one was activated. The simulation results indicate that the sprinkler location had a significant effect on the suppression of conveyor belt fires. The ventilation and the HRR played major roles in the determination of the activation time of the sprinkler. Although the ventilation was fixed, the HRR from the burning of the belt continually increased before the spray was on.

5.3. Effect of water flow rates

To develop more effective engineering designs for the fire suppression system in the belt entry, simulations were conducted to investigate the effect of water flow rate on the suppression of conveyor belt fires. 30 CFR Part 75.1101-8 requires that the water discharge rate from the sprinkler system shall not be less than 0.25 gallon per minute per square foot (10.2 liter per minute per square meter) of the top surface of the belt. Using the 15.2-m (50-ft) distance required for protecting the conveyor belt, the total required water flow rate is 284 liter per minute (Lpm) for the whole system if every sprinkler opens. This is an average of 36 Lpm per sprinkler if every sprinkler opens. The FSF water system is capable of supplying 750 Lpm—well above the requirement. In the test in the FSF, with one sprinkler activating, the water flow rate from that sprinkler was 207 Lpm. This water flow rate was enough to extinguish the belt fire.

In the simulations, with one sprinkler activating 2.4 m from the belt leading edge and the other inputs kept the same, the water flow rate was varied from 10 Lpm to 250 Lpm. It was found that the larger water flow rate had an insignificant effect on the suppression of the conveyor belt fires, as shown in Fig. 13. The HRR after sprinkler activation for the 250 Lpm water flow rate was only slightly lower than those for the water flow rates of 10Lpm, and 100Lpm.

The centerline belt surface temperatures 5 m from the belt leading edge for different water flow rates are plotted in Fig. 14. The surface temperatures were all reduced sharply with the activation of the sprinkler. With the larger water flow rate, the lower surface temperature was achieved because more water was hitting the surface to cool it. Fig. 15 shows the centerline surface temperatures 7 m from the belt leading edge for the different water flow rates. At the water flow rate of 10 Lpm, the surface temperature at this position was about 15 °C higher than the temperatures for other water flow rates. The surface temperatures were very close to each other for the other water flow rates.

Fig. 16 shows the effect of water flow rate on the smoke temperature 15 cm below the roof downstream of the belt structure. As the water flow rate increased, the smoke temperature after sprinkler activation was lower. Li and Ingason (2013) also observed that there is no significant difference in the effect of water flow rates on the fire development after sprinkler activation in the model-scale tunnel fire tests with automatic sprinklers.

These results indicate that the water flow rate has little effect on the fire suppression of conveyor belt fire as long as it is above a critical value, 25 Lpm, in this study. This is in good agreement with the regulations that require at least 36 Lpm, on average, if every sprinkler opens.

5.4. Effect of the activation temperature

Regulation 30 CFR Part 75.1101-8 requires that each individual sprinkler shall be activated at a temperature of not less than 150°F (65.6°C) and not more than 300°F (148.9°C). The activation temperature of the sprinklers used in the test was 140°C. In the simulations, sprinklers with the activation temperatures of 68°C, 79°C, and 93°C were also simulated in addition to 140°C. The sprinkler 2.4m from the belt leading edge was activated and other parameters were kept the same.

As expected, with the lower activation temperature, the sprinkler was activated earlier. The activation times for the different activation temperature are shown in Table 1. Fig. 17 shows the HRR for different activation temperatures. It was found that except for the simulation with an activation temperature of 140°C, the fire was not developed before the sprinkler activation for all other activation temperatures. Therefore, there was no apparent HRR reduction after the sprinkler activation. Fig. 18 shows the centerline surface temperature 5 m from the belt leading edge for different activation temperatures. The centerline surface temperatures 5 m from the belt leading edge were much lower than that for activation temperature of 140°C at the time of activation as shown in Table 1. Fig. 19 shows the centerline surface temperature 7 m from the belt leading edge for different activation temperatures. It is interesting to see that for the activation temperatures of 68°C, 79°C, and 93°C, the surface temperature actually increased slightly after the sprinkler activation. The smoke temperatures 15 cm below the roof downstream of the belt structure for different activation temperatures are shown in Fig. 20. For the lower activation temperatures, the smoke temperature started to increase slowly after an abrupt drop.

6. Conclusions

CFD simulations were conducted to model the water spray suppression of conveyor belt fires in a large-scale tunnel. The CFD model was calibrated based on large-scale test results. The CFD model was able to capture the major characteristics of the water spray suppression of the conveyor belt fires. The calibrated model was used to investigate the effects of sprinkler location, water flow rate, and activation temperature on the effectiveness of the water suppression of conveyor belt fires.

Simulation results demonstrate that the sprinkler location has a significant effect on the fire suppression through affecting the development of the fire. Two modes of fire suppression were found when the distance from the first sprinkler to the belt leading edge increased from 0.3 to 2.4m. With the sprinkler located at 0.3 m and 2.4 m from the belt leading edge, the fire was suppressed after it was well developed. Therefore, the suppression was more efficient. At these two locations, the activation times were the longest and the resulting HRRs before the sprinkler activation were the largest. At the sprinkler locations of 0.9 m, 1.2 m, 1.5 m, and 1.8 m, the fire was suppressed before it was well developed, but the surface temperature 7 m from the belt leading edge increased after the sprinkler activation. At sprinkler locations of 0.6 m and 2.1 m, the fire was suppressed before it was well developed, and the sprinkler activation times were shorter than those at the locations of 0.3 m and 2.4m.

The water flow rate has little effect on the suppression of the belt fires when the water flow rate is above a critical value, 25 Lpm. However, the larger water flow rate can reduce the downstream smoke temperature further. The sprinkler activation temperature has an important impact on the effectiveness of the suppression of belt fires. With lower activation temperatures, the fire was suppressed before it was well developed.

Acknowledgments

The authors wish to thank Rick Thomas and John Soles of Office of Mine Safety and Health Research for conducting the large-scale conveyor belt fire suppression test.

References

Blanchard E, Fromy P, Carlotti P, Boulet P, Desanghere S, Vantelon JP, Garo JP. Experimental and numerical study of the interaction between water mist and fire in an intermediate test tunnel. Fire Technol. 2013; 50:565–587.

Hua J, Kumar K, Khoo BC, Xue H. A numerical study of the interaction of water spray with a fire plume. Fire Saf J. 2002; 37:631–657.

Jenft A, Collin A, Boulet P, Pianet G, Breton A, Muller A. Experimental and numerical study of pool fire suppression using water mist. Fire Saf J. 2014; 67:1–12.

Lawson, JR.; Walton, WD.; Evans, DD. Measurement of droplet size in sprinkler sprays. National Bureau of Standards; 1988. NBSIR 88-3715

Li YZ, Ingason H. Model scale tunnel fire tests with automatic sprinkler. Fire Saf J. 2013; 61:298–313.

McGrattan K, Baum H, Rehm H. Large eddy simulation of smoke movement. Fire Saf J. 1998; 30:161–178.

McGrattan, KB.; Hostikka, S.; Floyd, JE.; Baum, H.; Rehm, R.; Mell, W.; McDermott, R. Fire Dynamics Simulator (version 5.5): Technical Reference Guide. National Institute of Standards and Technology; 2010. p. 1018-5.NIST Special Publication

Nmira F, Consalvi JL, Kaiss A, Fernandez-Pello AC, Porterie B. A numerical study of water mist mitigation of tunnel fires. Fire Saf J. 2009; 44:198–211.

Novozhilov V, Harvie DJE, Green AR, Kent JH. A computational fluid dynamics model of fire burning rate and extinction by water sprinkler. Combust Sci Technol. 1997; 123:227–245.

Novozhilov V, Moghtaderi B, Kent JH, Fletcher DF. Solid fire extinguishment by a water spray. Fire Saf J. 1999; 32:119–135.

Prasad K, Li C, Kailasanath K. Simulation of water mist suppression of small scale methanol liquid pool fires. Fire Saf J. 1999; 33:185–212.

Prasad K, Patnaik G, Kailasanath K. A numerical study of water mist suppression of large scale compartment fires. Fire Saf J. 2002; 37:569–589.

Rowland JH, Verakis H, Hockenberry MA, Smith AC. Effect of air velocity on conveyor belt fire suppression systems. Trans Soc Min Metall Expl. 2011; 328:493–501.

Sheppard, DT. Spray characteristics of fire sprinklers. National Institute of Standards and Technology; 2002. NIST GCR 02-838

Sikanen T, Vaari J, Hostikka S, Paajanen A. Modeling and simulation of high pressure water mist systems. Fire Technol. 2014; 50:483–504.

Teacoach KA, Rowland JH, Smith AC. Improvements in conveyor belt fire suppression systems for U.S. coal mines. Trans Soc Min Metall Explor. 2011; 328:502–506.

Teacoach KA, Thomas RA. Evaluation of novel fire suppression systems for conveyor belt fires in underground coal mines. Proceeding of the Seventh International Seminar on Fire & Explosion Hazards. 2013:453–462.

Trelles J, Mawhinney JR. CFD investigation of large scale pallet stack fires in tunnels protected by water mist systems. J Fire Prot Eng. 2010; 20:149–198.

U.S. Code of Federal Regulations. Title 30-Mineral Resources; Chapter I-Mine Safety and Health Administration. Department of Labor Subchapter O-Coal Mine Safety and Health; 2013. Part 75-Mandatory Safety Standards-Underground Coal Mines, Subpart L-Fire Protection

Vaari J, Hostikka S, Sikanen T, Paajanen A. Numerical simulations on the performance of water-based fire suppression systems. VTT Technol. 2012; 54

Yao B, Chow WK. Extinguishment of a PMMA fire by water spray with high droplet speeds. Int J Therm Sci. 2005; 44:410–419.

Yoon SS, Him HY, DesJardin PE, Hewson JC, Tieszen SR, Blanchat TK. Unsteady RANS modeling of water-spray suppression for large-scale compartment pool fires. At Spray. 2007; 17:1–45.

Yuan L, Mainiero RJ, Rowland JH, Thomas RA, Smith AC. Numerical and experimental study on flame spread over conveyor belts in a large-scale tunnel. J Loss Prev Process Ind. 2014; 30:55–62.

Fig. 1.
NIOSH Fire suppression facility.

Fig. 2.
Setup of conveyor belt and ignition gas burners.

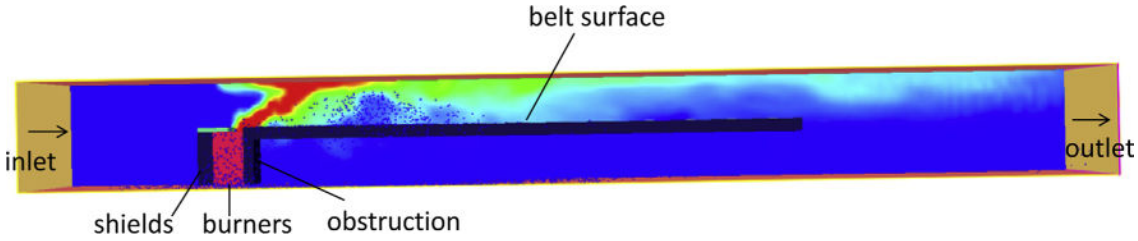

Fig. 3.
Physical model of simulated tunnel and conveyor belt.

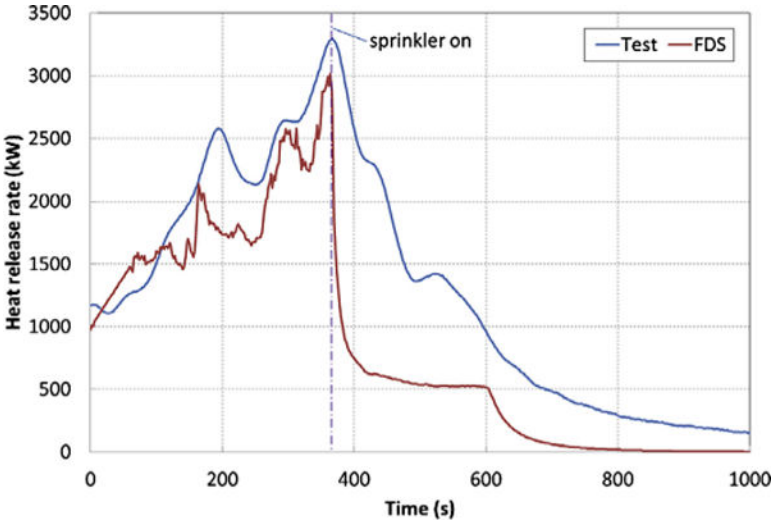

Fig. 4.
Comparison of heat release rates between test and simulation.

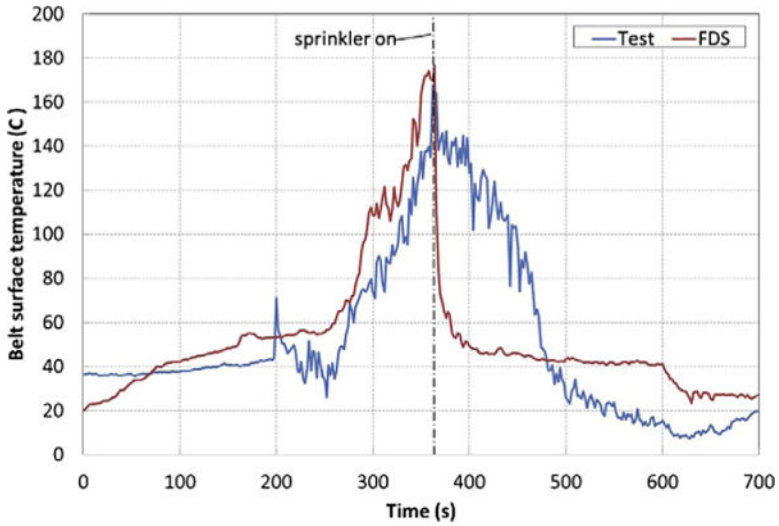

Fig. 5.
Comparison of surface temperatures between test and simulation.

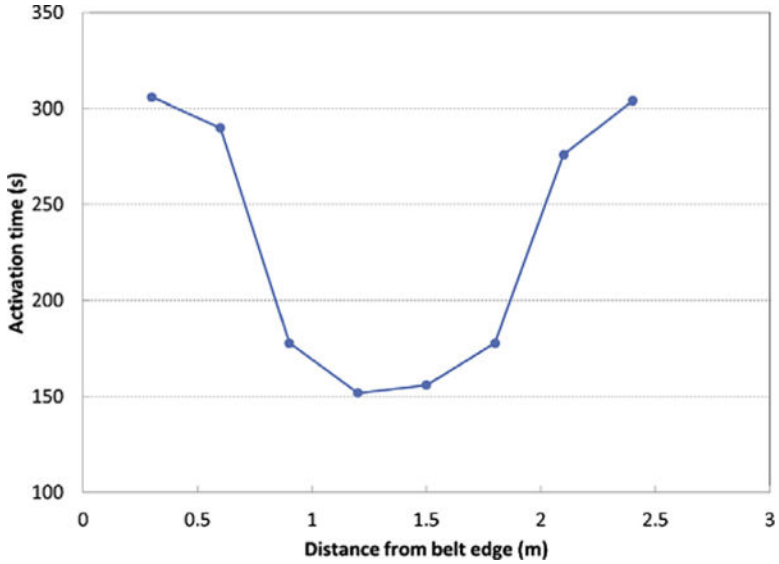

Fig. 6.
Activation times for the first sprinkler at different locations.

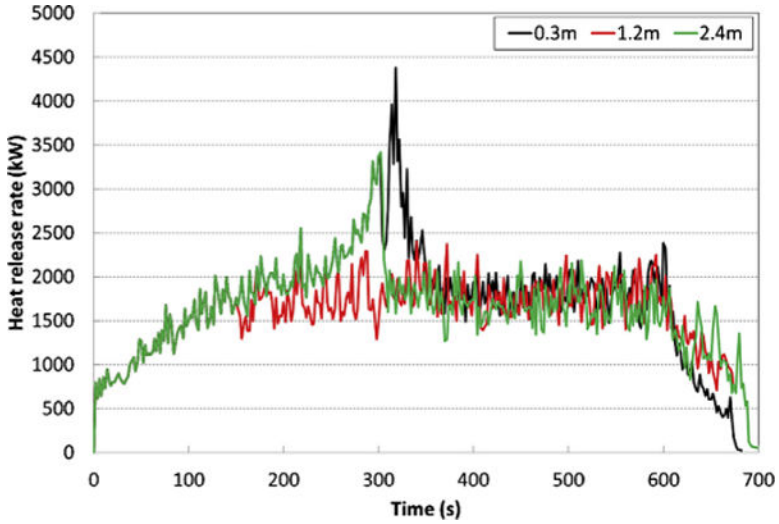

Fig. 7.
Heat release rates for different sprinkler locations.

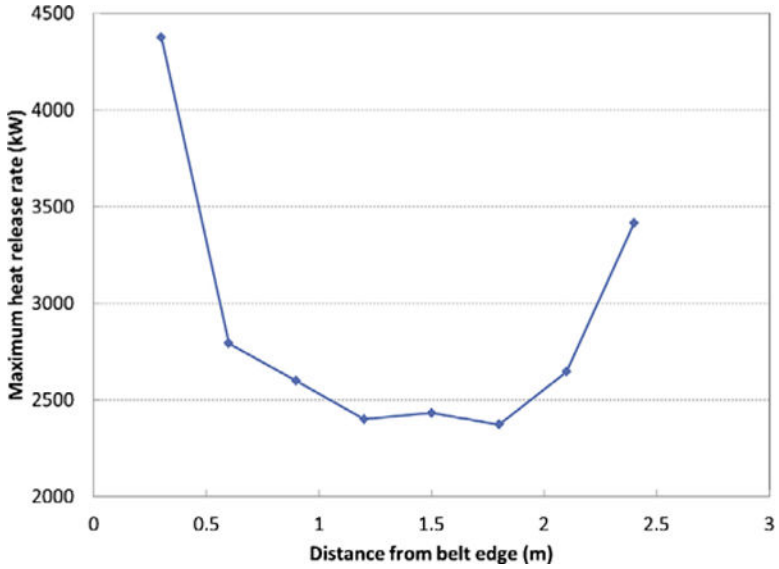

Fig. 8.
The maximum heat release rates before sprinkler activation for different.

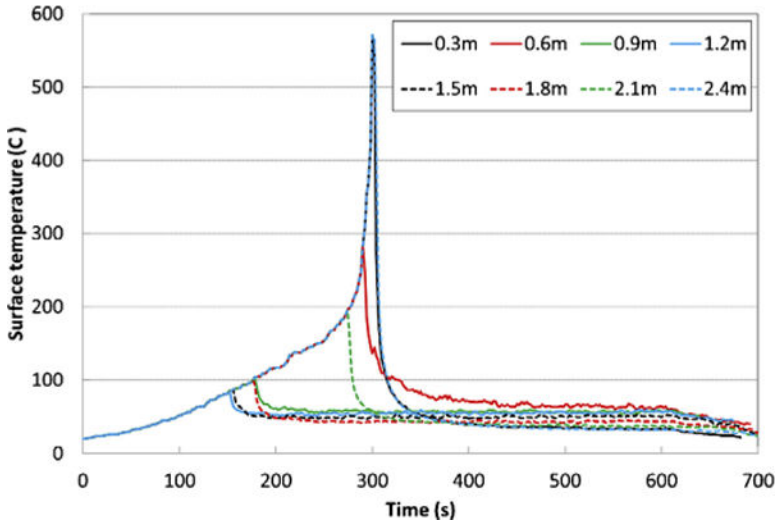

Fig. 9.

Belt surface temperatures 5 m from belt leading edge for different sprinkler locations. sprinkler locations.

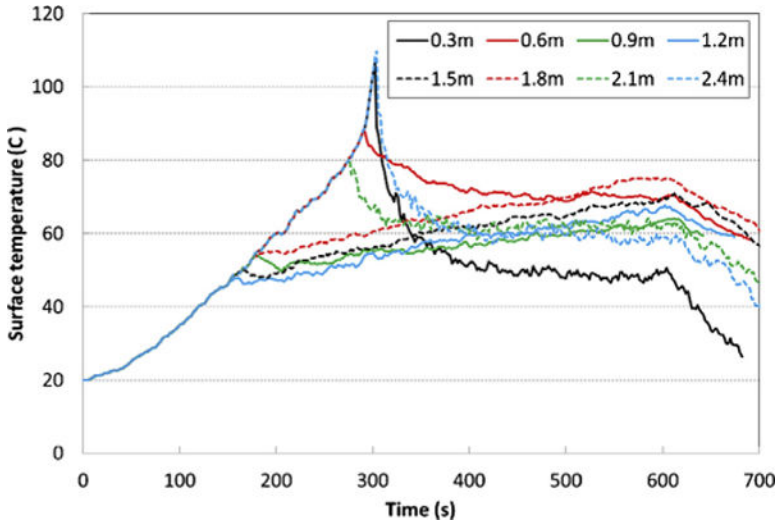

Fig. 10.
Belt surface temperatures 7 m from belt leading edge for different sprinkler locations.

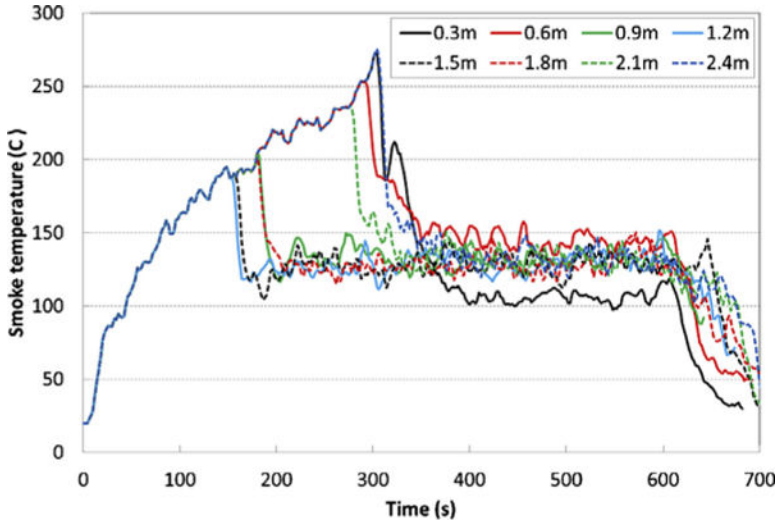

Fig. 11.

Downstream smoke temperatures 15 cm below roof for different sprinkler locations.

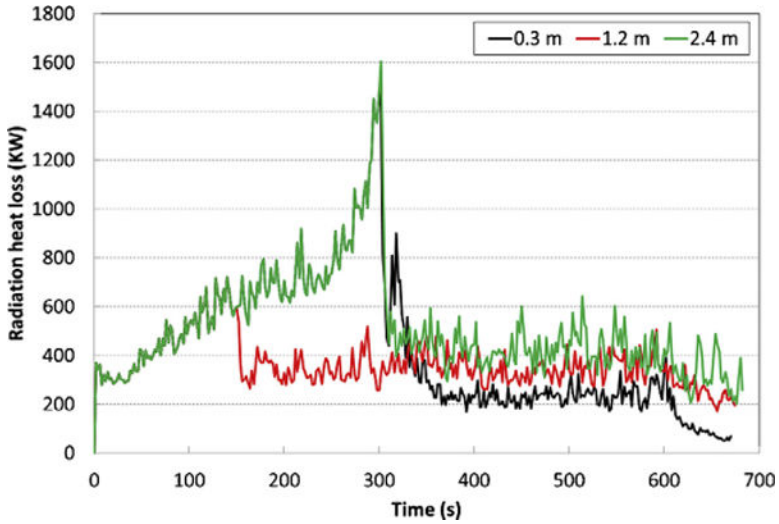

Fig. 12.
Radiation heat loss for different sprinkler locations.

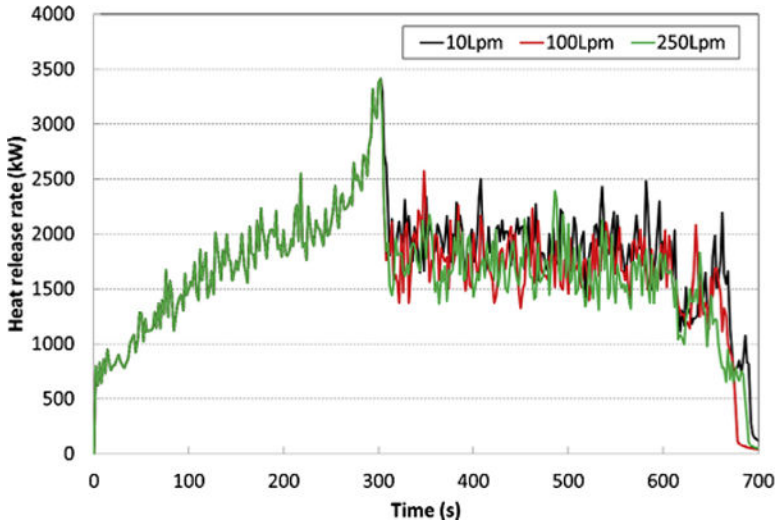

Fig. 13.
Heat release rates for different water flow rates.

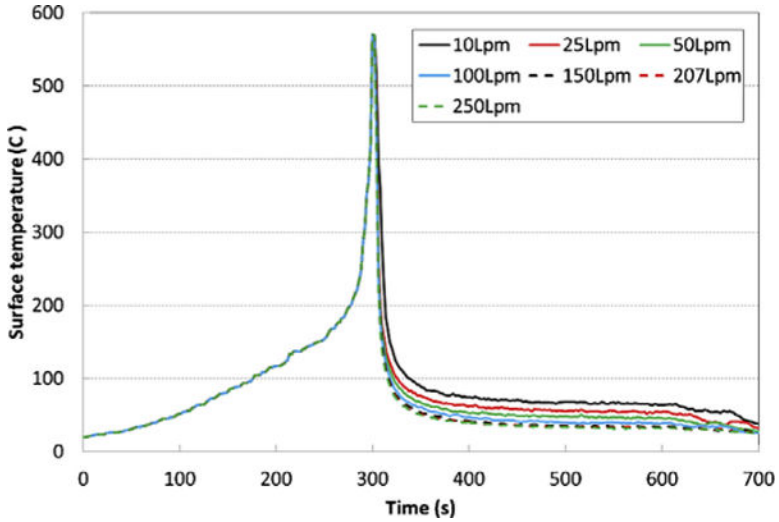

Fig. 14.

Belt surface temperatures for different water flow rates: 5 m from belt leading edge.

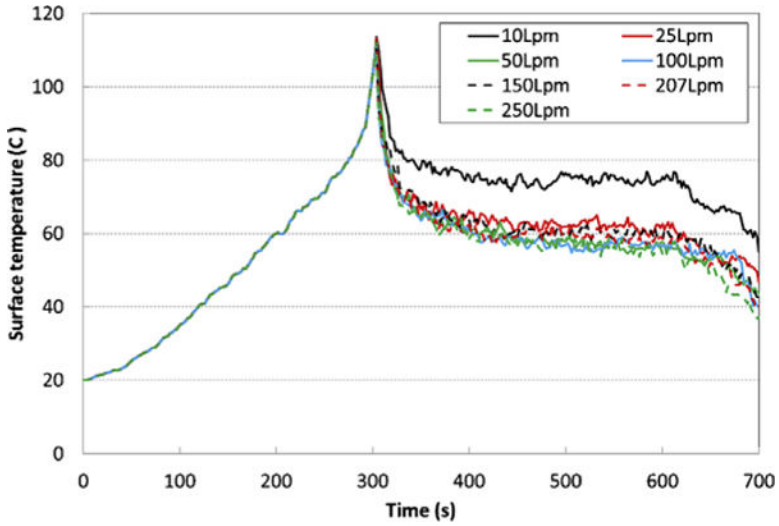

Fig. 15.
Belt surface temperatures for different water flow rates: 7 m from belt leading edge.

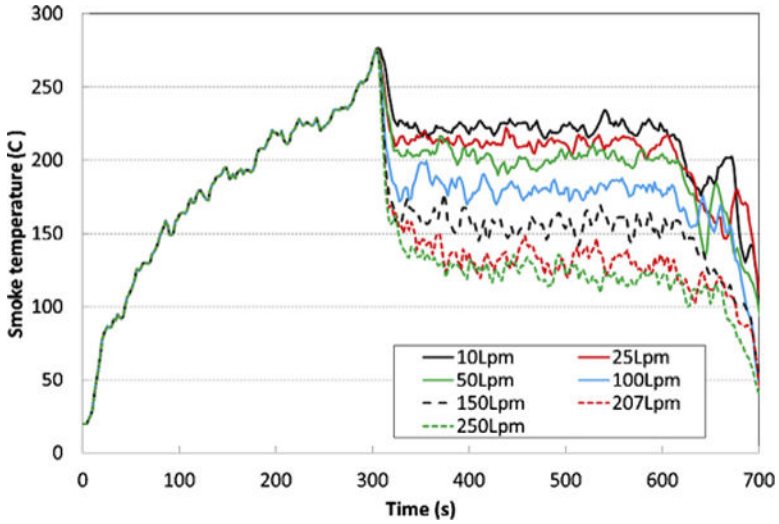

Fig. 16.

Downstream smoke temperatures 15 cm below roof for different water flow rates.

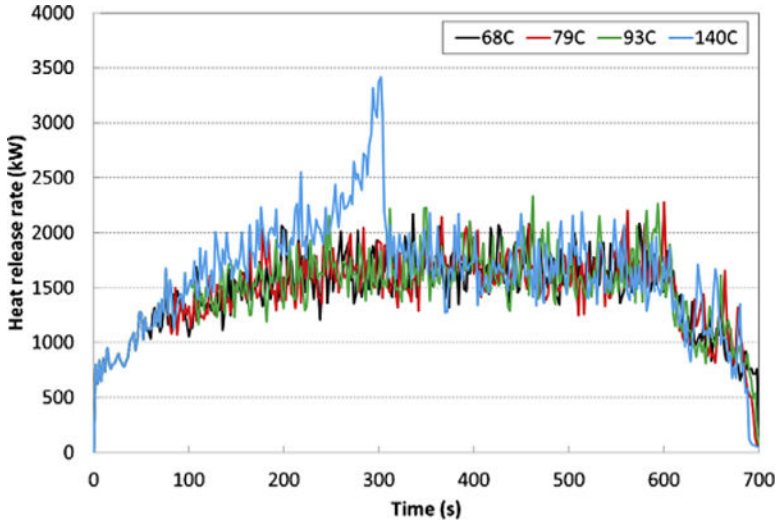

Fig. 17.
Heat release rates for different activation temperatures.

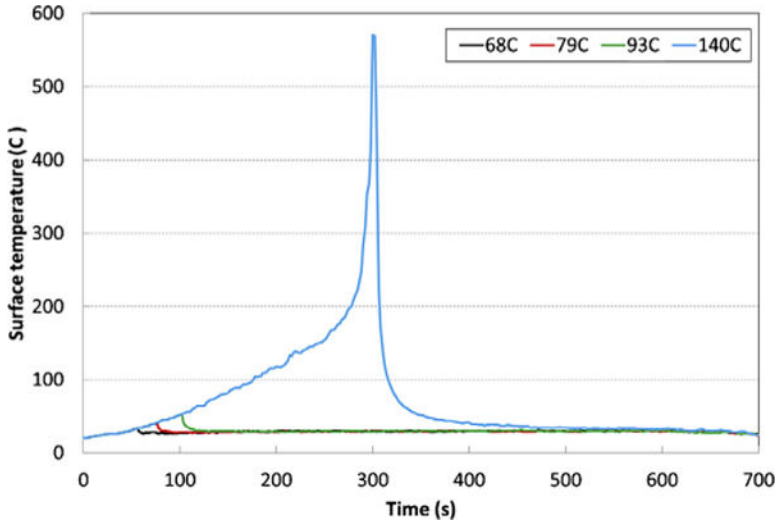

Fig. 18.

Belt surface temperatures 5 m from belt leading edge for different activation temperatures.

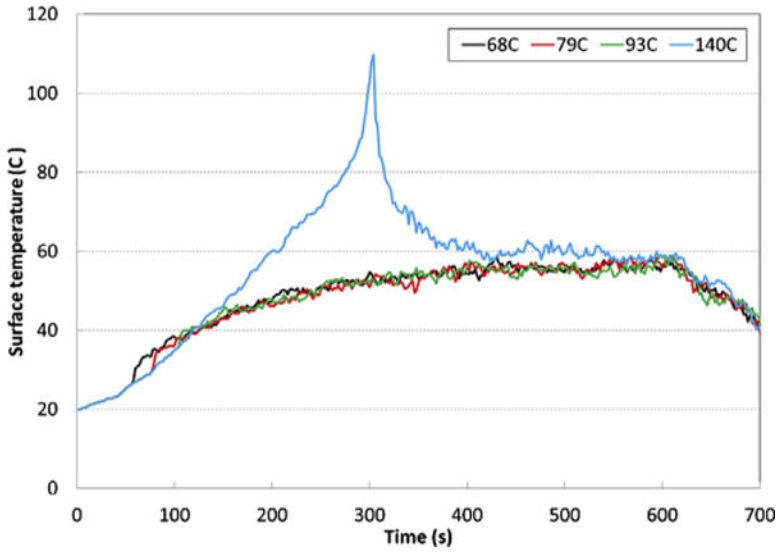

Fig. 19.

Belt surface temperatures 7 m from belt leading edge for different activation temperatures.

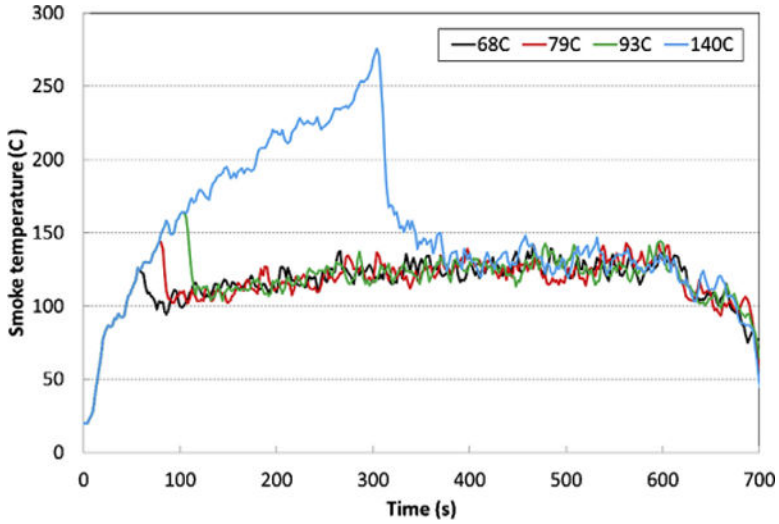

Fig. 20.

Downstream smoke temperatures 15 cm below roof for different activation temperatures.

Table 1

Sprinkler activation times and surface temperatures at activation.

Activation temperature (°C)	68	79	93	140
Activation time (s)	56	76	102	304
Surface temperature at activation (°C)	33	40	52	569